



Published in final edited form as:

Mater Des. 2021 January 1; 197: . doi:10.1016/j.matdes.2020.109249.

Effects of systematically varied thiourethane-functionalized filler concentration on polymerization behavior and relevant clinical properties of dental composites

S.H. Lewis^a, Fugolin APP^a, S. Lam^b, C. Scanlon^a, J.L. Ferracane^a, C.S. Pfeifer^{a,*}

^aOregon Health & Science University, Department of Restorative Dentistry, Biomaterials and Biomechanics, United States of America

^bApprenticeships in Science and Engineering (ASE, Saturday Academy), United States of America

Abstract

Introduction of thiourethane (TU) oligomer to resin-based dental restorative materials reduces stress and improves fracture toughness without compromising conversion. Localization of TU at the resin-filler interface via silanization procedures may lead to more substantial stress reduction and clinical property enhancements. The objective of this study was to evaluate composite properties as a function of TU-functionalized filler concentration. TU oligomers were synthesized using click-chemistry techniques and subsequently silanized to barium glass filler. Resin-based composites were formulated using varying ratios of TU-functionalized filler and conventional methacrylate-silanized barium filler. Material property testing included thermogravimetric analysis, real-time polymerization kinetics and depth of cure, polymerization stress, stress relaxation and fracture toughness. Clinical property testing included water sorption/solubility, composite paste viscosity, and gloss and surface roughness measured before and after subjecting the samples to 6 h of continuous tooth brushing in a custom-built apparatus using a toothpaste/water mixture. Increasing TU-filler in the composite resulted in as much as a 78% reduction in stress, coupled with an increase in fracture toughness. Conversion was similar for all groups. After simulated tooth brushing, gloss reduction was lower for TU-containing composites and surface roughness was less than or equal to the control.

Graphical Abstract

This is an open access article under the CC BY-NC-ND license (<http://creativecommons.org/licenses/by-nc-nd/4.0/>).

*Corresponding author at: 2730 South Moody Ave, Portland, OR 97201, United States of America. pfeiferc@ohsu.edu (C.S. Pfeifer). CRediT authorship contribution statement

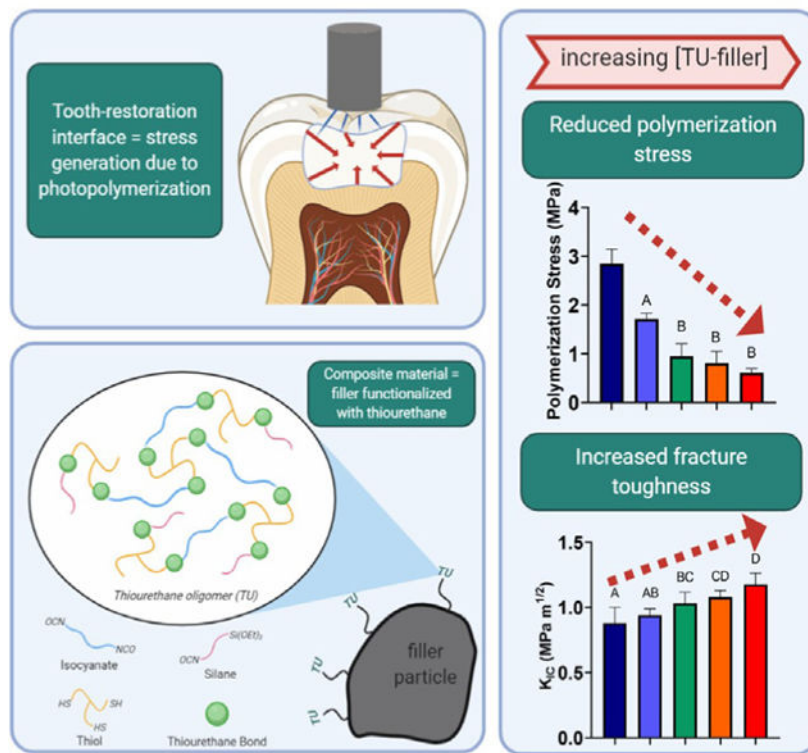
S.H. Lewis: Data curation, Formal analysis, Methodology, Writing - original draft. **Fugolin APP:** Data curation, Formal analysis, Methodology, Writing - review & editing. **S. Lam:** Data curation, Formal analysis, Methodology. **C. Scanlon:** Data curation, Formal analysis, Methodology. **J.L. Ferracane:** Writing - review & editing. **C.S. Pfeifer:** Conceptualization, Data curation, Formal analysis, Funding acquisition, Project administration, Resources, Supervision, Writing - review & editing.

Declaration of Competing Interest

The authors declare that they have no known competing financial interests or personal relationships that could have appeared to influence the work reported in this paper.

Appendix A. Supplementary data

Supplementary data to this article can be found online at <https://doi.org/10.1016/j.matdes.2020.109249>.



Keywords

Dimethacrylates; Thiourethane oligomers; Dental composites; Polymerization stress; Fracture toughness; Surface properties

1. Introduction

Inorganic filler silanization is a common strategy for enhancing mechanical properties of composites by creating covalent bonds between the filler and organic matrix. Use of silanized filler particles in dental composites has been shown to improve flexural, tensile and compressive strength compared to composites formulated without silane coupling agents [1–3]. 3-(trimethoxysilyl)propyl methacrylate (MPS) is a common silane compound, which provides the inorganic filler with surface-tethered methacrylate functionality. However, the relative stiffness of the MPS molecule, coupled with the potential for hydrolytic ester degradation, suggest materials modified with this compound will be challenged by conditions *in vivo* [3,4]. This type of mono-functional silane has been shown to form a mono-layer at the filler surface, and therefore, the covalent interaction with the monomer matrix in the composite occurs in a relatively constrained space [5,6]. Interfacial stresses are generated as the matrix monomers polymerize and shrink away from the highly rigid filler to which they are bonded [1,7]. In fact, fractographic studies have suggested that crack propagation is facilitated at this interface [8]. Fortunately, advances in silane chemistry have resulted in a wide variety of multi-functional, crosslinking and hyperbranched oligomeric silanes which have been shown to provide many benefits, including reduced polymerization

shrinkage stress, resistance to degradation and wear, improved fracture toughness, enhanced viscoelastic stress relaxation and self-healing capabilities [4,8,9]. The mechanism through which stress reduction and mechanical reinforcement are achieved is believed to be associated with the increased compliance and mobility of the covalent bonds between the inorganic filler and the organic resin matrix [7,10].

Another avenue for reinforcing the resin-filler interface is through the introduction of thiourethane (TU) additives. These pre-polymerized, high molecular weight oligomers have demonstrated value when incorporated into the organic matrix of dental composites, providing reduced polymerization stress, enhanced conversion and improved mechanical properties [11]. More recently, this type of chemistry has gained attention for its potential to provide stress relaxation via trans-thiocarbonylation and heat-catalyzed thiol-thiourethane exchange reactions [12,13]. One drawback to the approach is that the addition of TU to the matrix monomers significantly affects the viscosity of the resultant material. Thus, a possible solution is to incorporate the TU into the composite via silane functionality to provide a direct attachment to the filler particles. Synthesized using simple and scalable click-chemistry techniques, TUs are viable candidates for filler surface functionalization by incorporating a methoxy silane moiety [14]. This has the potential to not only reduce the viscosity effects seen in matrix-modified TU systems, but also to maximize the benefits of TUs by creating an efficient stress transfer system localized at the matrix-filler interface, where it is needed the most. Previous studies have demonstrated that the use of TU-silanes leads to decreased polymerization stress and increased fracture toughness in highly filled composites at a single concentration [14,15]. This approach may find application in several fields beyond dental restoratives, including coatings, self-healing materials and renewable/reprocessable materials [12,13,16].

The objectives of this study were to evaluate the effects of varying the proportions of TU-silanized filler and conventional methacrylate-silanized filler on reaction kinetics, polymerization stress, mechanical properties and other clinically relevant properties of resin-based composites. The tested hypotheses were: 1) Increasing the proportion of TU-silanized filler in the composites will result in enhanced degree of conversion, fracture toughness, depth of cure and reduced polymerization stress. Furthermore, other properties, including gloss, surface roughness, handling/viscosity and water sorption/solubility will not be negatively affected by the TU-modified fillers. 2) Selective targeting of the resin-filler interface via TU filler silanization will result in improved performance compared with previously reported studies examining the effects of incorporating TU into the matrix phase of dental composites [11,17].

2. Materials and methods

2.1. Thiourethane synthesis and filler particle functionalization

All chemicals were purchased from Sigma Aldrich (Milwaukee, WI, USA) at 97% purity or greater and used as received, unless otherwise stated. Thiourethanes (TU; TMP:HDMI-NCO-Si) were synthesized as described previously using a 2.5:1:1 M ratio of trimethylol-tris-3-mercaptopropionate (TMP), dicyclohexylmethane 4,4'-diisocyanate (HDMI) and 3-

(triethoxysilyl)propyl isocyanate (NCO-Si) [14]. The completed reaction was confirmed by the disappearance of the isocyanate peak (mid-IR, 2270 cm^{-1}) and verified by ^1H NMR.

Neat, unfunctionalized silica glass filler (barium-alumino silicate, $0.7\text{ }\mu\text{m}$ average particle size, Schott Dental Glass, Landshut, Germany) was TU-functionalized as previously described [2,14]. Briefly, synthesized TU was added at 2.0 wt% to a solution of aqueous ethanol (80 vol%, pH 4.5, adjusted using 1 M acetic acid) plus neat glass filler and stirred for 24 h at room temperature. The solution was then filtered, washed with hexanes, and dried for 4 days at $37\text{ }^\circ\text{C}$. Methacrylate-silanized barium-alumino silicate fillers were utilized in control and experimental composite formulations and were obtained from the same commercial source described above.

Filler silanization efficiency was quantified using thermogravimetric analysis (TGA; TA Instruments, New Castle, DE, USA). Filler samples (15 mg) were subjected to a heating ramp from 50 to $850\text{ }^\circ\text{C}$ at $10\text{ }^\circ\text{C}/\text{min}$ and the percent mass remaining was recorded as a function of temperature ($n = 3$).

2.2. Composite composition

Resin-based composites were formulated using an organic matrix composed of bisphenol-A-diglycidyl dimethacrylate, urethane dimethacrylate and triethylene glycol dimethacrylate at a 50:30:20 mass ratio (BUT; Esstech, Essington, PA, USA). Camphorquinone and ethyl-4-dimethylaminobenzoate (CQ/EDMAB) were added at 0.2 and 0.8 wt%, respectively, as the photoinitiators and butylated hydroxy toluene (BHT) was incorporated as a stabilizer at 0.2 wt%. Total inorganic filler content was 70% by weight, of which 5 wt% was Aerosil OX50 fumed silica (Evonik Industries, Essen, Germany) and 95 wt% was $0.7\text{ }\mu\text{m}$ silica glass filler, providing composition similar to a micro-hybrid composite. The $0.7\text{ }\mu\text{m}$ silica glass filler was functionalized with TMSP (3-(trimethoxysilyl)propyl methacrylate, control) and TU-silane in various proportions. Table 1 summarizes the groups according to the weight ratios of methacrylate-silanized and TU-silanized fillers.

All photocuring experiments were conducted using an LED curing light (DEMI Plus, Kerr Dental, Brea, CA, USA), fitted with a 8 mm diameter light guide, with a maximum output irradiance of $600\text{ mW}/\text{cm}^2$, verified using an external power meter (Moletron, Portland, OR, USA). The irradiance values reaching the surface of the specimen in each test condition are detailed below.

2.3. Photopolymerization reaction kinetics and degree of conversion

Photopolymerization reaction kinetics were measured using real-time near-infrared spectroscopy (Nicolet 6700, ThermoFisher Scientific, Madison, WI, USA) with 10 mm diameter specimens cast between glass slides using a 0.8 mm spacer. Samples ($n = 3$) were photocured for 20 s with the LED light at a distance of 1 cm from the surface of the sample delivering an irradiance of $150\text{ mW}/\text{cm}^2$. This relatively low irradiance was selected here to highlight differences among the materials, mainly due to a limitation of the data acquisition of the method (2 data points per second). The degree of conversion was monitored for 180 s and was calculated based on the change in area of the methacrylate vinyl absorbance peak (6165 cm^{-1}) [18].

2.4. Polymerization stress

A single-cantilever beam apparatus (Bioman) was used to assess polymerization stress in real time. Uncured composite was situated in a 0.8 mm gap between a silica glass plate and a 5 mm diameter steel piston connected to a load cell. The piston was roughened using 600 grit silicon carbide paper and treated with metal primer (Z-Prime Plus, Bisco Inc., Schaumburg, IL, USA), while the glass plate was surface treated with silane to promote adhesion during curing (Ceramic Primer, 3 M ESPE, St. Paul, MN, USA). The specimens were photopolymerized through the glass for 60 s at an incident irradiance of 560 mW/cm². Calibrated load signal (N) and cantilever beam displacement (μm) data were collected for 300 s. Polymerization stress was calculated at each time point and the final stress value was reported as the average of 5 specimens.

2.5. Composite depth of cure - 2D mapping

Composite bars were prepared using a 2 × 2 × 5 mm deep silicone mold sandwiched between glass slides and photopolymerized for 60 s at 560 mW/cm² on the top surface, then stored dry for 7 days in the dark. Subsequently, the specimens were removed from the molds, embedded in epoxy resin and cut longitudinally into 0.5 mm thick slices using a diamond saw (Accutom-5, Struers, Cleveland, OH, USA). The slices were then mounted on glass slides and conversion was mapped at 10 discrete sample depths (5 mm total depth, $n = 3$) using an IR microscope (Nicolet Continuum, Nicolet 6700, ThermoFisher Scientific, Madison, WI, USA). Conversion was calculated using the same method described above with the inclusion of the aromatic peak area at 4625 cm⁻¹ as an internal reference to normalize for small differences in specimen thickness.

2.6. Composite rheological properties

Composite paste viscosity was measured using a TA Instruments DHR-1 rheometer (TA Instruments, New Castle, DE, USA). Rheological tests were performed using 8 mm parallel plate geometry and a gap thickness of 300 μm. Shear rate sweeps were carried out at 25 °C from 1 to 100 s⁻¹. Average viscosity was determined based on values that were within the linear deformation range.

To further elucidate viscosity effects contributed by the incorporation of TU-silanized filler, additional composites were formulated without OX-50 fumed silica at a ratio of 1:1 between the organic matrix and inorganic filler particles. Viscosity measurements ($n = 3$) were conducted using the same rheometer settings described above. The materials were used shortly after mixing, and inspected prior to use to ensure even distribution of fillers.

The storage modulus (G') and loss modulus (G'') crossover time point (time to gel point) was measured on the rheometer using 20 mm parallel disc plates at a frequency of 10 Hz and 0.01% strain. An equipped “Smart Swap” photo accessory allowed for real-time measurement of modulus development during photopolymerization. Samples were purged with nitrogen for 5 min prior to testing and throughout the duration of the test in order to minimize oxygen inhibition at the specimen boundary. Photopolymerization was conducted using a mercury arc lamp with an irradiance of 100 mW/cm² (320–500 nm) for 5 min

(Acticure 4000, EXFO, Montreal, Canada). This light source was used in this experiment because the smart swap accessory is designed to fit its light guide only.

2.7. Fracture toughness

Single-edge notched beam specimens ($5 \times 2 \times 25$ mm) were used to measure the fracture toughness (K_{IC}) of composites in accordance with ASTM Standard E399–90. Samples were prepared in steel molds held between glass slides and photocured for 80 s per side at 600 mW/cm² (Demi LED). Based on the spot size of the curing light at the surface of the sample, the bar was cured at 4 equally-spaced segments per side for 20 s each. A centrally-located, 2.5 mm length razor blade was used to create a single-edge notch on one longitudinal side of the bar. Fracture tests ($n = 6$) were carried out after 7 day dry storage in the dark, using a universal testing machine in three-point bending configuration with a crosshead speed of 0.5 mm/min (MTS Criterion, Eden Prairie, MN, USA). K_{IC} was calculated using eq. (1) where P is fracture load (N), L , W , B are the specimen length, width and thickness, respectively (mm), and a is the notch length (mm).

$$K_{IC} = \frac{3PL}{2BW^{3/2}} \left\{ 1.93 \left(\frac{a}{W} \right)^{1/2} - 3.07 \left(\frac{a}{W} \right)^{3/2} + 14.53 \left(\frac{a}{W} \right)^{5/2} - 25.11 \left(\frac{a}{W} \right)^{7/2} + 25.80 \left(\frac{a}{W} \right)^{9/2} \right\} \quad (1)$$

2.8. Stress relaxation

Stress relaxation experiments were conducted using dynamic mechanical analysis (Q800 DMA, TA Instruments, New Castle, DE, USA). Composite bar specimens ($1 \times 3 \times 25$ mm) were cured for 90 s per side at 600 mW/cm² and thermally post-cured at 180 °C until >90% conversion was reached in order to prevent additional polymerization during DMA testing. Stress relaxation measurements were performed in tension mode at discrete temperature points between 80 and 155 °C using a fixed 0.05% strain. The relaxation modulus decrease was measured for 30 min per temperature point. The characteristic relaxation time was defined as the time required for the material to relax to 50% of the original modulus, E_0 .

2.9. Water sorption and solubility

Reaction kinetics specimens ($n = 3$) were stored dry for 7 days in the dark and then used to evaluate the effect of TU-filler concentration on water sorption (W_{sp}) and solubility (W_{sl}) according to ISO 4049. Specimen masses were recorded (m_1) prior to water storage (5 mL). After one week, specimens were removed, excess water was dried with absorbent paper and masses were recorded (m_2). Subsequently, specimens were dried to a stable mass under vacuum desiccation (m_3). Eqs. (2), (3) were used to calculate (W_{sp}) and (W_{sl}), where V_0 is the specimen volume ($2\pi r^2 h$):

$$W_{SP} = \frac{(m_2 - m_1)}{V_0} \quad (2)$$

$$W_{SL} = \frac{(m_3 - m_1)}{V_0} \quad (3)$$

2.10. Gloss and roughness after tooth brush simulation

Simulated tooth brushing was conducted using a novel mechanical brushing system to assess the effect of TU concentration on composite gloss and surface roughness. Fracture toughness bar specimens ($5 \times 2 \times 12.5$ mm) were mounted in epoxy resin 7 days after testing. The specimens were then subjected to finishing (1 min) and polishing (1 min) using the Enhance PoGo finishing system (Dentsply Sirona, York, PA, USA). The epoxy-mounted samples were attached to an acrylic plate driven by a DC gear motor the tooth brushing simulator (Fig. 1). A toothpaste solution consisting of one tube of Crest Pro-Health Toothpaste (130 g) and 390 mL of water was prepared and added to the reservoir. A stationary Oral-B Sensi-soft Ultra Soft toothbrush was mounted such that the specimens rotated through the toothpaste and then against the brush (approx. force of 100 g) at a frequency of one brush/s for a total of 6 h.

The tooth brushing simulation time was determined to be roughly equivalent to 90 days of normal brushing exposure on a tooth/tooth restoration. A conservative estimate was used of one minute of brushing per tooth per day. The brushing stroke rate in the oral cavity was estimated to be 4 strokes per second, or 240 strokes per minute. Therefore, 4 min on the tooth brush simulator was approximately equivalent to the daily brushing exposure of one tooth. Thus, 360 min of simulated brushing was roughly equivalent to 90 days of manual tooth brushing.

Composite gloss and surface roughness measurements were taken prior to brushing and every 90 min thereafter until the simulation was complete. Gloss ($n = 3$; GU units) was measured with a glossmeter with 60° geometry and a 2×2 mm measurement area (Novo-Cure, Rhopoint Instrumentation, East Sussex, UK). Surface roughness ($n = 3$; Ra, μm) was measured using a surface profilometer with a tracing length of 2 mm and a 0.8 mm cutoff.

2.11. Statistical analysis

Data was analyzed using one-way ANOVA, with Tukey's test used for multiple comparisons ($\alpha = 0.05$). For gloss and surface roughness data, a two-way ANOVA and Tukey's test was used for comparisons between groups at selected time points. Regression analyses were utilized to investigate connections between TU content and polymerization stress as well as TU content and fracture toughness.

3. Results

3.1. Filler characterization

According to the thermogravimetric analysis mass loss profiles shown in Fig. 2 the MA-silane control filler lost approximately 4.2 wt%, while the TU-silanized filler lost 12.6 wt%. A comparison of the volume fraction (calculated using the TGA mass loss results) versus weight fraction of resin, inorganic filler and MA and/or TU silane for each of the composite

groups is shown in Table 2. In total, the 0.7 μm barium filler accounted for 66.5 wt% and between 46.0 and 49.7 vol% of the total composite composition. The TU silane volume fraction varied from 4.0 to 15.0 vol% in the groups containing TU-functionalized filler, while the MA silane volume fraction made up between 1.2 and 5.1 vol%.

3.2. Photopolymerization kinetics and conversion

Photopolymerization conversion reached at least 50% for all composites and there was no statistical difference in final degree of conversion between the control and experimental groups (Fig. 3). The maximum rate of polymerization ($R_{p\text{max}}$) was reduced in accordance with increasing TU filler concentration (linear regression, $r^2 = 0.91$). $R_{p\text{max}}$ for the 100% TU group was reduced by 48.1% compared to the 100% MA control ($5.0 \pm 0.2\% \text{ s}^{-1}$ vs $2.6 \pm 0.4\% \text{ s}^{-1}$; Fig. 4B). The time required to reach $R_{p\text{max}}$ was delayed in the experimental groups in relation to increasing TU content (Fig. 4A).

Fig. 5 shows R_p plotted versus conversion, and illustrates the systematic suppression of polymerization rate as a function of increasing TU concentration. The plots also demonstrate that the degree of conversion at $R_{p\text{max}}$ was not statistically different from the 100% MA control.

3.3. Polymerization stress

Photopolymerization stress was significantly reduced for all TU-containing groups (Fig. 6). Stress for the composite with 25% TU-modified filler was reduced by 39.8% compared to the 100% MA control group ($1.7 \pm 0.1 \text{ MPa}$ vs $2.9 \pm 0.3 \text{ MPa}$). The groups containing 50, 75 and 100% TU-modified filler were all statistically similar, but all showed a dramatic stress reduction versus the control, with a maximum of a 78.3% reduction seen in the 100% TU group ($0.6 \pm 0.1 \text{ MPa}$ vs $2.9 \pm 0.3 \text{ MPa}$). The final stress values showed an exponential decrease relative to increasing TU-filler concentration ($R^2 = 0.94$; Fig. 6B).

3.4. Fracture toughness

With the exception of the 25% TU material, fracture toughness increased by a significant amount for all groups relative to the control (Fig. 7). The greatest increase was observed in the 100% TU group, which showed a 33.6% improvement in fracture toughness compared to the control ($0.9 \pm 0.1 \text{ MPa}\cdot\text{m}^{1/2}$ vs $1.2 \pm 0.1 \text{ MPa}\cdot\text{m}^{1/2}$). A linear relationship between TU-filler concentration and fracture toughness was observed ($R^2 = 0.99$).

3.5. Gloss and surface roughness

Gloss values for all composites decreased during simulated tooth brushing (Fig. 8A). Pre-brushing gloss units ranged from $75.6 \pm 6.5 \text{ GU}$ (100% MA) to $84.8 \pm 3.5 \text{ GU}$ (25% TU) and there was a significant difference between the control (100% MA) and both 25% TU and 50% TU groups. At the conclusion of the tooth brushing simulation (time = 360 min), all experimental groups containing TU-modified filler showed significantly higher gloss values than the control, with the greatest difference observed between 100% MA ($18.5 \pm 3.4 \text{ GU}$) and 75% TU ($41.8 \pm 5.2 \text{ GU}$). The greatest gloss reduction was seen for the control (75.5% reduction), while the 75% TU material saw the least reduction at 47.7%.

The surface roughness of the composites increased throughout the duration of the simulated brushing experiment for all groups and, in general, groups with higher TU content showed a less dramatic increase in roughness (Fig. 8B). Pre-brushing roughness values were between $0.062 \pm 0.020 \mu\text{m}$ and $0.144 \pm 0.082 \mu\text{m}$ for the 25% TU group and 100% MA control, respectively. After 360 min of simulated tooth brushing, the highest absolute roughness value was seen in the control ($0.330 \pm 0.090 \mu\text{m}$), while the 100% TU group had both the lowest roughness value ($0.183 \pm 0.055 \mu\text{m}$) and the lowest relative change in roughness (approximately a 2.2-fold increase in roughness). Gloss and roughness correlation plots pre- and post-brushing are included in Appendix A: Supplementary Data (Figs. 1 and 2). A strong correlation was observed between gloss and surface roughness prior to the simulated brushing, although the correlation did not track with increasing TU-filler concentration. Post-brushing gloss and surface roughness did not have a strong correlation, for reasons discussed in the following sections.

3.6. Water sorption and solubility

There was no statistical difference between the groups for water sorption (W_{SP}) or water solubility (W_{SL}), as shown in Fig. 9. W_{SP} ranged between 18.6 ± 0.9 and $23.9 \pm 3.2 \mu\text{g}/\text{mm}^3$, while W_{SL} ranged between 3.7 ± 1.8 and $8.0 \pm 2.8 \mu\text{g}/\text{mm}^3$.

3.7. Rheological properties

The viscosity results for all groups of composites with the formulation consisting of 70 wt% total filler and 30 wt% matrix resin are shown in Fig. 10A. The results did not follow a consistent trend, with the 50% TU group having the highest viscosity ($6.6\text{E}4 \pm 1.1\text{E}4 \text{ Pa}\cdot\text{s}$) and the 75% TU group having the lowest average viscosity ($1.4\text{E}3 \pm 5.6\text{E}2 \text{ Pa}\cdot\text{s}$). The 25% TU and 75% TU groups were statistically similar to the control, while the 50% TU and 100% TU groups had significantly higher average viscosities.

Fig. 10B displays the viscosity results for composites formulated using only the MA or TU-silanized fillers at a 50 wt% loading level. This test was conducted in an attempt to isolate the effects of the silane-treated fillers without the presence of fumed silica. It is important to highlight that the materials were inspected after use to ensure the fillers were kept in suspension. The results of this test showed a statistically higher average viscosity for the 100% MA control group ($26.2 \pm 1.1 \text{ Pa}\cdot\text{s}$) compared to the 25% TU, 50% TU and 75% TU groups (20.4 ± 1.8 , 21.8 ± 1.3 and $21.5 \pm 0.4 \text{ Pa}\cdot\text{s}$, respectively). The 100% TU material had the highest average viscosity for this formulation, at $30.3 \pm 1.3 \text{ Pa}\cdot\text{s}$.

Dynamic rheological properties of the composites were measured during polymerization and the time at which the crossover modulus occurred ($\tan \delta = 1$) is shown in Fig. 11. The average crossover time was greater in groups with the highest amount of TU filler (50% TU, 75% TU and 100% TU). These groups experienced more than a two-fold increase in the time to crossover compared to the 100% MA control (up to $13.4 \pm 1.4 \text{ s}$ for 100% TU versus $6.0 \pm 1.2 \text{ s}$ for 100% MA). The 25% TU group had the lowest crossover time at $4.3 \pm 0.8 \text{ s}$, but was not statistically different from the control.

3.8. Stress relaxation

Viscoelastic stress relaxation results are shown in Fig. 12 for all groups. The characteristic relaxation time was defined as that required for the material to relax to 50% of the original modulus, E_0 . Relaxation times were plotted as a function of the temperatures at which the relaxation tests were performed (80, 95, 110, 125, 140 and 155 °C). In general, the TU-containing materials showed consistently faster relaxation times compared to the methacrylate-based control up to 125 °C. At that temperature, 100% TU had an average relaxation time of 2.2 ± 0.2 min, while the 100% MA control group had a relaxation time of 10.7 ± 5.9 min; a reduction of nearly 80%. The only exception was observed at the highest temperature evaluated here, at which 100% TU had similar relaxation time to the methacrylate, which was slower than the other TU-containing groups.

3.9. Composite depth of cure - 2D mapping

Fig. 13 shows a 2D heatmap of composite degree of conversion at increasing sample depth for each of the groups. In general, higher degrees of conversion were observed in groups with greater TU filler concentrations. Both the conversion at the surface of the samples and the conversion throughout the depth of the sample remained higher for the composites with 50% TU, 75% TU and 100% TU as compared to the 100% MA control in. The exception was the 25% TU group, which displayed markedly lower conversion throughout. This group achieved a maximum conversion of only 51.8% compared to 63.5% for the control and 73.7% for the 100% TU group.

4. Discussion

This study evaluated thiourethane-functionalized fillers at systematically varied ratios in relation to control methacrylate silane fillers in regards to clinically-relevant properties. Covalent attachment of TU to the filler particle surface resulted in concentration-dependent reductions in $R_{p_{max}}$ and polymerization stress, as well as significant increases in fracture toughness and overall improvements in cure depth. Furthermore, improvements in gloss and surface roughness after simulated tooth brushing were seen in relation to the control, indicating better ability to maintain polish. Water sorption and solubility were unaffected by the addition of TU fillers and composite paste viscosity was seen to increase primarily only at high TU concentrations. These differences were consistent with part one of our hypothesis that TU filler silanization improves physical and mechanical properties of dental composites.

Filler silanization efficiency, as assessed by TGA (Fig. 2), as well as the composite mass and volume fraction calculations reported in Table 2 showed that the total silane mass was approximately 3 times greater for TU-silanized filler versus MA-silanized filler. This is due primarily to the higher molecular weight TU silane compared to the MA silane (approximately 5000 g/mol for TU silane versus 248 g/mol for 3-(trimethoxysilyl)propyl methacrylate) [17]. Additionally, the TU oligomer contains multiple triethoxysilane functional groups, whereas the MA silane has single trimethoxysilane functionality. This, combined with inherent flexibility of the TU oligomer, likely results in the TU molecule having multiple covalent $\equiv\text{Si}-\text{O}-\text{Si}\equiv$ bonds per filler particle [20]. This could lead to non-

uniform, and potentially multilayered TU surface coverage as opposed to monolayer coverage of the methacrylate-based silane [6].

The mass loss differential between TU and MA silanized filler particles resulted in variations in effective filler weight and volume fractions of the composites, highlighted in Table 2. For example, the total filler volume fraction for 100% MA was 62.3%, but only 57.1% for 100% TU. The filler volume fraction increased monotonically as the TU-filler concentration decreased. It has been shown that polymerization stress is inversely related to filler content and fracture toughness is proportional to filler volume fraction [21,22]. From this, an increase in shrinkage stress due to the increase in volume of organic matrix, as well as compromised mechanical properties could have been expected for the TU-containing composites [2]. In fact, the opposite was observed: significant increases in fracture toughness and decreases in polymerization stress were seen in all TU-containing groups (Figs. 6 and 7), which will be discussed in greater detail later. This indicated that beneficial aspects afforded by TU silanization, such as delayed gelation and vitrification via chain-transfer of thiols to vinyls and network toughening due to flexible, high molecular weight TU oligomers, were sufficient to overcome the reduced filler volume fraction compared to the MA-based control composite [14]. Table 2 also shows that TU concentrations in the 100% TU and 75% TU groups were approximately 6.3 and 8.4 wt%, respectively. These values are comparable to the overall TU concentrations used in previous studies (6 wt%) [23].

According to Figs. 4 and 5, the polymerization rate was slower and $R_{p_{max}}$ was suppressed in groups containing TU-modified filler, but the overall final degree of conversion was not significantly different from the control. Previous studies using TU either in the matrix or on the filler surface have shown moderate increases in final conversion compared to conventional methacrylate-based composites [15]. Chain transfer reactions from TU pendant thiols to vinyls in the matrix delay gelation and postpone the onset of vitrification. This effectively delays the diffusional limitations to propagation and generally is expected to result in higher final conversion [24]. Conversion at $R_{p_{max}}$ also followed the conversion results (Fig. 5B), showing no significant differences between the groups. Trailing ends of the conversion-dependent polymerization rate curves, corresponding to deceleration, showed reduced slopes in TU-containing groups, which is consistent with behavior seen in systems containing small molecule thiol additives [25]. Therefore, it was somewhat surprising that the final degree of conversion was not higher in the groups with TU-filler. One explanation could be related to the presence of the OX50 fumed silica, which has a high surface-area-to-volume ratio. This may have caused additional mobility restrictions during polymer network formation and counteracted chain transfer effects near the end of vitrification, thus limiting the final degree of conversion. It is also possible that the relatively low curing energy used here, coupled with the somewhat lower rate of polymerization for the TU-containing groups, did not allow for higher conversions to be achieved. For this reason, the depth of cure experiments, intended to mimic clinical conditions, were carried out with specimens cured at higher irradiance. In those instances, as will be discussed below, the conversion values surpassed 70% for the experimental materials.

Although the presence of TU-functional fillers did not affect the degree of conversion in disc specimens, Fig. 13 showed an enhanced cure depth in specimens 10 mm in length in 50% TU, 75% TU and 100% TU composites. Differences in conversion at the surface were also noted for this test, with the higher TU concentrations showing significantly higher conversions versus the control. The conversion differences were more marked in this case, which was likely due to the longer curing time at higher irradiance, compared to the reaction kinetics polymerization conditions (5 min @ 600 mW/cm² versus 20 s @ 150 mW/cm²). While the 100% MA control had a conversion at the surface of 62.5% and a reduction of 8.3% at 10 mm, the 75% TU group had a surface conversion of 77.1% and a reduction of only 5.5% at 10 mm. Previous studies have shown that incorporation of TU into the matrix improved both refractive index and cure depth of composite specimens, which was consistent with these findings, with the exception of the 25% TU group [26]. Since filler size and refractive index play an important role in light attenuation, scattering and transmission during polymerization, it is likely that the lower conversion seen in the 25% TU group could be the result of a refractive index mismatch between the TU filler and the MA filler [27]. The effects of TU additives on light transmission are currently being investigated and will be reported separately.

Polymerization shrinkage stress reduction via modification of the matrix/filler interface has been studied extensively [28,29]. When inorganic filler contains methacrylate surface functionalization, stress accumulates at the interface due to differences in thermal expansion during polymerization and the moduli disparity between the compliant matrix and low-compliance inorganic filler [7]. For example, Feng, et al., have shown that polymerization contraction stresses cause the matrix resin to pull away from the filler surface, both in constrained and non-constrained conditions [8]. As opposed to developing low-shrink, pre-polymerized resin additives which have the potential to significantly increase viscosity and limit the ability to maximize inorganic filler loading, particle surface modification achieves the goal of stress reduction by selectively targeting regions of highest stress concentration. In this study, an exponential decrease in stress was observed in relation to TU-filler concentration (Fig. 6B). The 100% TU composite had a stress reduction of more than 78% compared to the 100% MA control composite (0.6 ± 0.1 vs 2.9 ± 0.3 MPa), despite having approximately 6.5 vol% less inorganic filler (Table 2). Stress reduction in these systems is due in large part to delayed gelation from thiol chain transfer during polymerization [11,25]. Furthermore, it is likely that having flexible, high molecular weight TU oligomer as a covalent connection between the resin and filler minimizes interfacial stress buildup by accommodating free volume changes during the polymerization process [30]. To support the idea of thiol chain transfer inducing delayed gelation in these systems, Fig. 11 illustrated that the crossover modulus occurred at a later time point in groups with higher TU-filler concentrations. The crossover time point, where $\tan \delta = 1$, is generally accepted as being near the critical gel point [31,32]. The conversion at that point was not measured in this study, but it is hypothesized that the TU-containing materials had progressed further in conversion at the time the crossover was detected, based on previous literature with small molecule thiols [25]. Thus, it is likely that the presence of TU in the composite postpones the impact of diffusion limitations to propagation, delaying the buildup of stress and resulting in substantially lower overall stress, as shown in Fig. 6 [11,25].

Comparison of stress reduction in composites with TU-modified matrix versus TU tethered to the filler particles further highlights the importance of localizing thiourethane at the matrix/filler interface. Previously, it has been shown that a maximum of approximately 20 wt% TU can be added to the matrix (equivalent to approximately 6 wt% of the overall composite) before mechanical properties and handling characteristics become compromised [11]. Experimental composites that had 20 wt% TU in the matrix, achieved a maximum stress reduction of 57% compared to a control containing no TU [23]. Interestingly, when the TU was instead tethered to the filler surface at a similar concentration, the relative stress reduction was 72% (6.3 wt% TU concentration for the 75% TU group). These results support part two of the hypothesis that TU filler silanization improves properties and performance compared to matrix-dispersed TU. This finding has a potentially significant impact on the design of novel materials, and may find application in several different fields, such as biomedical engineering and paint and coatings industries.

In addition to TU-functionalized fillers reducing stress *during* polymerization, Fig. 12 illustrates the apparent differences in *long-term* stress relaxation behavior of composites formulated with TU-functional fillers. Faster relaxation times were observed in nearly all TU-containing composites and at a majority of the tested temperatures when composite bar specimens were held at a fixed 0.05% strain for 30 min. Recently, it has been demonstrated that excess thiol within a TU-based network can participate in dynamic exchange reactions, leading to network rearrangement and subsequent relaxation of accumulated stresses within the polymer network [9,12,13,33]. Although the temperatures at which the DMA tests were conducted are not clinically practical, testing at elevated temperatures, at or near the T_g , may provide an accelerated method for discerning the aforementioned dynamic adaptability of TU-modified composites [13,33,34]. It should be noted that sample variation within some of the groups were high and may have been the result of inherent network heterogeneity within the composite. Temperature-dependent stress relaxation measurements using DMA are accurate when testing thermo-rheologically simple, homogeneous, unfilled polymer networks [35]. However, specimen variation within groups may be exacerbated when testing heterogeneous composites or materials which can undergo conformational network changes as a result of thiol exchange reactions [13,36].

Similarly, the mechanical properties obtained by fracture toughness tests revealed increased K_{IC} values in proportion to TU-filler concentration (Fig. 7). Filler silanization with TU oligomers showed up to a 34% increase in fracture toughness (100% TU group). It has been reported previously that the addition of TU to the matrix of dental composites increased fracture toughness by as much as 38% [11]. These results are not surprising and suggest the possibility of strong interfacial bonding at the matrix/filler interface as a result of flexible thiocarbamate bonds contributed by the TU oligomer, enabling more efficient energy dissipation/absorption during crack propagation [11,37]. In addition, the ability for stress relaxation to occur within the bulk of the vitrified network can potentially function as a crack deflection mechanism and provide enhanced toughness. The stress relaxation data complements the fracture toughness results and suggests that TU-containing materials may be effective in accommodating sustained stresses that are present in the bulk composite post-polymerization and at the bonded interface of high c-factor, direct dental restorations [38].

In addition to these more fundamental polymer network properties, this study also investigated the effect of TU filler silanization on several other clinically relevant properties of dental composites: viscosity, water sorption/solubility, gloss and surface roughness retention. Incorporation of TU into the matrix phase has previously been shown to increase paste viscosity and affect composite handling at moderate to high concentrations [11]. This is to be expected when portions of the organic matrix are substituted with high molecular weight, high hydrogen bonding-potential, prepolymerized oligomer [4,11]. These characteristics can limit the ability to incorporate higher concentrations of inorganic filler, thereby compromising mechanical properties. Fig. 10 suggests that optimization of the TU-filler concentration can result in similar or potentially even reduced viscosity when compared to the MA control composite. Interestingly, there was not a correlation between viscosity and TU-filler concentration, suggesting that interparticle interactions between the OX50, MA-filler and TU-filler play an important role in the overall viscosity of the composite. For example, in Fig. 10A, the 50% TU group had a viscosity nearly tenfold higher than the 100% MA group. However, in Fig. 10B, where the OX50 variable was removed, the viscosity was more than 15% lower than the MA-silanized control group. The high surface area-to-volume ratio of the OX50 allows for infiltration in and around the larger MA and TU-silanized filler particles and may have a greater influence on uniform dispersion of filler particles throughout the composite. If particle dispersion is non-uniform, there could be regions where aggregation of filler occurs and thus results in a higher measured viscosity. The average interparticle spacing for composites containing 50 wt% filler was calculated using Eq. 2, where D_s is the particle spacing (μm), D_p is the average filler particle size (μm) and V_p is the filler volume fraction (%). The interparticle spacing increased linearly with increasing TU filler content and resulted in approximately a 20% increase in spacing between the 100% MA and 100% TU groups (1.35 μm and 1.62 μm , respectively). It is likely that this increase in interparticle spacing resulted in lower measured viscosities for the 25% TU, 50% TU and 75% TU groups, relative to the 100% MA control. A possible explanation for the viscosity increase seen in the 100% TU group is that the particle surface coverage of the higher molecular weight, long-chain TU oligomers at this loading level was substantial enough to counteract the effects of the increased interparticle distance. In other words, the filler particles may have exhibited extended “reach” such that particle-particle interactions were more prevalent between TU molecules on adjacent filler particles [39].

$$D_S = \frac{2D_P(1 - V_P)}{3V_P} \quad (4)$$

Prior studies with TU-matrix-modified composites have shown reduced water solubility compared to unmodified counterparts [15]. This was likely due to both an increase in overall conversion in the TU systems, which reduced the amount of extractable unreacted monomer, and also because of restricted small-molecule diffusion caused by the presence of high molecular weight TU oligomers [15]. In this study, however, neither water sorption nor water solubility were affected by the presence of TU-filler (Fig. 9). This was somewhat expected based on the fact that there was not a significant difference in degree of conversion between the groups.

To date, little work has been done to investigate the effect of thiourethanes on surface polish retention under simulated tooth brushing in vitro. A novel brushing system was utilized in this study that allowed for 6 h of continuous tooth brushing of multiple specimens, which equated to more than 90 days of manual tooth brushing. As expected, gloss reductions and surface roughness increases were observed for all groups, at each 90-min measured time interval (Fig. 8). However, the relative gloss reduction and change in surface roughness was consistently lower in the groups with high TU-filler concentrations. Furthermore, the absolute surface roughness for the 100% TU group never surpassed 0.2 μm , previously reported as a critical threshold for increased bacterial retention and plaque deposition [40,41]. Additionally, the initial surface roughness values (pre-brushing) were up to 57% lower than for the control. This could be due to enhanced network homogeneity afforded by the introduction of the TU-silane fillers [11]. The flexible, high molecular weight TU oligomers also impart a toughening effect on the composites which may contribute to abrasion resistance and lower surface roughness after brushing. Gloss is a complex material property that depends on a variety of factors including filler size, distribution and refractive index, mechanical properties, and matrix viscosity and refractive index [42–44]. The refractive index of the TU likely played a role in the lower gloss reduction seen in the TU-modified composites compared to the control, since systems modified with TU have been shown to increase polymer refractive index [26]. However, in this prior study, the refractive index increase was limited to systems without OX50. When OX50 (with a relatively low RI = 1.45) was incorporated, a refractive index mismatch was apparent and resulted a lower composite conversion depth of cure. Nevertheless, this study highlighted that gloss decreased at a lower rate in the composites containing TU-silane fillers. Therefore, it is hypothesized that the toughness contributed by the TU additives, localized at the resin-filler interface, may be effective at limiting deterioration of the composite during simulated long-term brushing. It is also worth noting that increased TU-filler content resulted in marginally lower overall filler weight and volume fractions (Table 2), which may help to explain the higher initial and final gloss observed in these groups. The effects of these compositions on the long-term occlusal wear is unknown and should be investigated in a future study.

5. Conclusions

The addition of TU-functionalized inorganic fillers to dental resin-based composites resulted in systematic reductions in polymerization stress and increased fracture toughness without affecting the degree of conversion. Composites modified with TU-fillers withstood the deleterious effects of prolonged tooth brushing under simulated conditions and showed reduced surface roughness and lower gloss reduction compared to composites formulated with standard methacrylate-silane treated fillers. Selective targeting of the resin-filler interface utilizing TU-functional fillers produced low stress, high performance dental materials, making them viable candidates for numerous clinical use applications.

Supplementary Material

Refer to Web version on PubMed Central for supplementary material.

Acknowledgements

The authors thank NIH-NIDCR for funding (U01-DE023756; K02-DE025280; R01-DE026113) the Apprenticeships in Science and Engineering program (ASE) from Saturday Academy for support to Shirley Lam, and the OHSU School of Dentistry, office of the dean, for the scholarship to Conor Scanlon.

References

- [1]. Aydıno lu A, Yoruç ABH, Effects of silane-modified fillers on properties of dental composite resin, *Mater. Sci. Eng. C* 79 (2017) 382–389, 10.1016/j.msec.2017.04.151.
- [2]. Lung CYK, Matinlinna JP, Aspects of silane coupling agents and surface conditioning in dentistry: an overview, *Dent. Mater* 28 (2012) 467–477, 10.1016/j.dental.2012.02.009. [PubMed: 22425571]
- [3]. Matinlinna J, Özcan M, Lassila L, Kalk W, Vallittu P, Effect of the cross-linking silane concentration in a novel silane system on bonding resin-composite cement, *Acta Odontol. Scand* 66 (2008) 250–255, 10.1080/00016350802247131. [PubMed: 18622831]
- [4]. Fronza BM, Rad IY, Shah PK, Barros MD, Giannini M, Stansbury JW, Nanogel-based filler-matrix interphase for polymerization stress reduction, 2019.
- [5]. Ochsmann JW, Lenz S, Lellig P, Emmerling SGJ, Golriz AA, Reichert P, You J, Perlich J, Roth SV, Berger R, Gutmann JS, Stress-structure correlation in ps-pmma mixed polymer brushes, *Macromolecules*. 45 (2012) 3129–3136, 10.1021/ma2025286.
- [6]. Matinlinna JP, Lung CYK, Tsoi JKH, Silane adhesion mechanism in dental applications and surface treatments: a review, *Dent. Mater* 34 (2018) 13–28, 10.1016/j.dental.2017.09.002. [PubMed: 28969848]
- [7]. Ye S, Azarnoush S, Smith IR, Cramer NB, Stansbury JW, Bowman CN, Using hyperbranched oligomer functionalized glass fillers to reduce shrinkage stress, *Dent. Mater* 28 (2012) 1004–1011, 10.1038/jid.2014.371. [PubMed: 22717296]
- [8]. Feng L, Suh BI, Shortall AC, Formation of gaps at the filler-resin interface induced by polymerization contraction stress. Gaps at the interface, *Dent. Mater* 26 (2010) 719–729, 10.1016/j.dental.2010.03.004. [PubMed: 20621775]
- [9]. Huang Z, Wang Y, Zhu J, Yu J, Hu Z, Surface engineering of nanosilica for vitrimer composites, *Compos. Sci. Technol* 154 (2018) 18–27, 10.1016/j.compscitech.2017.11.006.
- [10]. Tang S, Lo TY, Horton JM, Bao C, Tang P, Qiu F, Ho RM, Zhao B, Zhu L, Direct visualization of three-dimensional morphology in hierarchically self-assembled mixed poly(tert-butyl acrylate)/ polystyrene brush-grafted silica nanoparticles, *Macromolecules*. 46 (2013) 6575–6584, 10.1021/ma401264m.
- [11]. Bacchi A, Pfeifer CS, Rheological and mechanical properties and interfacial stress development of composite cements modified with thio-urethane oligomers, *Dent. Mater* 32 (2016) 978–986, 10.1016/j.dental.2016.05.003. [PubMed: 27257101]
- [12]. Gamardella F, Guerrero F, De la Flor S, Ramis X, Serra A, A new class of vitrimers based on aliphatic poly(thiourethane) networks with shape memory and permanent shape reconfiguration, *Eur. Polym. J* 122 (2020) 109361, 10.1016/j.eurpolymj.2019.109361.
- [13]. Li L, Chen X, Torkelson JM, Reprocessable polymer networks via thiourethane dynamic chemistry: recovery of cross-link density after recycling and proof-of-principle solvolysis leading to monomer recovery, *Macromolecules*. 52 (2019) 8207–8216, 10.1021/acs.macromol.9b01359.
- [14]. Faria-e-Silva AL, dos Santos A, Tang A, Giroto EM, Pfeifer CS, Effect of thiourethane filler surface functionalization on stress, conversion and mechanical properties of restorative dental composites, *Dent. Mater* 34 (2018) 1351–1358, 10.1016/j.dental.2018.06.023. [PubMed: 29934126]
- [15]. Borges MG, Barcelos LM, Menezes MS, Soares CJ, Fugolin APP, Navarro O, Huynh V, Lewis SH, Pfeifer CS, Effect of the addition of thiourethane oligomers on the sol-gel composition of BisGMA/TEGDMA polymer networks, *Dent. Mater* (2019) 1–9, 10.1016/j.dental.2019.07.015. [PubMed: 31500904]

- [16]. Jin K, Li L, Torkelson JM, Recyclable crosslinked polymer networks via one-step controlled radical polymerization, *Adv. Mater* 28 (2016) 6746–6750, 10.1002/adma.201600871. [PubMed: 27206061]
- [17]. Bacchi A, Dobson A, Ferracane JL, Consani R, Pfeifer CS, Thio-urethanes improve properties of dual-cured composite cements, *J. Dent. Res* 93 (2014) 1320–1325, 10.1177/0022034514551768. [PubMed: 25248610]
- [18]. Stansbury JW, Dickens SH, Determination of double bond conversion in dental resins by near infrared spectroscopy, *Dent. Mater* 17 (2001) 71–79, 10.1016/S0109-5641(00)00062-2. [PubMed: 11124416]
- [19]. Cabosil Safety Data Sheet, Free. Manuf. Supply Co <https://www.freemansupply.com/msds/combined/fillers/cabosil.pdf> 2015.
- [20]. Fugolin AP, Sundfeld D, Ferracane JL, Pfeifer CS, Toughening of dental composites with thiourethane-modified filler interfaces, *Sci. Rep* 9 (2019) 1–9, 10.1038/s41598-019-39003-w. [PubMed: 30626917]
- [21]. Ferracane JL, Berge HX, Condon JR, In vitro aging of dental composites in water - effect of degree of conversion, filler volume, and filler/matrix coupling, *J. Biomed. Mater. Res* 42 (1998) 465–472, 10.1002/(SICI)1097-4636(19981205)42:3<465::AID-JBM17>3.0.CO;2-F. [PubMed: 9788511]
- [22]. Gonçalves F, Kawano Y, Braga RR, Contraction stress related to composite inorganic content, *Dent. Mater* 26 (2010) 704–709, 10.1016/j.dental.2010.03.015. [PubMed: 20378161]
- [23]. Bacchi A, Yih JA, Platta J, Knight J, Pfeifer CS, Shrinkage / stress reduction and mechanical properties improvement in restorative composites formulated with thiourethane oligomers, *J. Mech. Behav. Biomed. Mater* 78 (2018) 235–240, 10.1016/j.jmbbm.2017.11.011. [PubMed: 29175492]
- [24]. Lovell LG, Berchtold KA, Elliott JE, Lu H, Bowman CN, Understanding the kinetics and network formation of dimethacrylate dental resins, *Polym. Adv. Technol* 12 (2001) 335–345, 10.1002/pat.115.
- [25]. Pfeifer CS, Wilson ND, Shelton ZR, Stansbury JW, Delayed gelation through chain-transfer reactions: mechanism for stress reduction in methacrylate networks, *Polymer (Guildf)*. 52 (2011) 3295–3303, 10.1016/j.polymer.2011.05.034. [PubMed: 21799544]
- [26]. Faria-e-Silva AL, Pfeifer CS, Impact of thio-urethane additive and filler type on light-transmission and depth of polymerization of dental composites, *Dent. Mater* 33 (2017) 1274–1285, 10.1016/j.dental.2017.07.020. [PubMed: 28807329]
- [27]. Shortall AC, Palin WM, Burtscher P, Refractive index mismatch and monomer reactivity influence composite curing depth, *J. Dent. Res* 87 (2008) 84–88, 10.1177/154405910808700115. [PubMed: 18096900]
- [28]. Amdjadi P, Ghasemi A, Najafi F, Nojehdehian H, Pivotal role of filler/matrix interface in dental composites: review, *Biomed. Res. An Int. J. Med. Sci* 28 (2017).
- [29]. Davidson C, Feilzer A, Polymerization shrinkage and polymerization shrinkage stress in polymer-based restoratives, *J. Dent* 25 (1997) 435–440. [PubMed: 9604575]
- [30]. Miguel A, De La Macorra JC, A predictive formula of the contraction stress in restorative and luting materials attending to free and adhered surfaces, volume and deformation, *Dent. Mater* 17 (2001) 241–246, 10.1016/S0109-5641(00)00077-4. [PubMed: 11257297]
- [31]. Winter HH, Can the gel point of a cross-linking polymer be detected by the $G' - G''$ crossover? *Polym. Eng. Sci* 27 (1987) 1698–1702, 10.1039/c3cs60235d.
- [32]. Fairbanks BD, Schwartz MP, Bowman CN, Anseth KS, Photoinitiated polymerization of PEG-diacrylate with lithium phenyl-2,4,6-trimethylbenzoylphosphinate: polymerization rate and cytocompatibility, *Biomaterials*. 30 (2009) 6702–6707, 10.1016/j.biomaterials.2009.08.055. [PubMed: 19783300]
- [33]. Sowan N, Dobson A, Podgorski M, Bowman CN, Dynamic covalent chemistry (DCC) in dental restorative materials: implementation of a DCC-based adaptive interface (AI) at the resin–filler interface for improved performance, *Dent. Mater* 36 (2020) 53–59, 10.1016/j.dental.2019.11.021. [PubMed: 31810600]

- [34]. Lei M, Yu K, Lu H, Qi HJ, Influence of structural relaxation on thermomechanical and shape memory performances of amorphous polymers, *Polymer (Guildf)*. 109 (2017) 216–228, 10.1016/j.polymer.2016.12.047.
- [35]. Menczel JD, Prime RB, *Thermal Analysis of Polymers: Fundamentals and Applications*, 2008 10.1002/9780470423837.
- [36]. Vaidyanathan TK, Vaidyanathan J, Cherian Z, Extended creep behavior of dental composites using time-temperature superposition principle, *Dent. Mater* 19 (2003) 46–53, 10.1016/S0109-5641(02)00009-X. [PubMed: 12498896]
- [37]. Sun CJ, Wu W, Mahanti S, Sadeghipour K, Baran G, Debnath S, Finite element analysis of toughening for a particle-reinforced composite, *Polym. Compos* 27 (2006) 360–367, 10.1002/pc.
- [38]. Watts DC, Satterthwaite JD, Axial shrinkage-stress depends upon both C-factor and composite mass, *Dent. Mater* 24 (2008) 1–8, 10.1016/j.dental.2007.08.007. [PubMed: 17920115]
- [39]. Spanoudakis J, Young RJ, Crack propagation in a glass particle-filled epoxy resin, *J. Mater. Sci* 19 (1984) 473–486.
- [40]. Bollen CML, Papaioanno W, Van Eldere J, Schepers E, Quirynen M, Van Steenberghe D, The influence of abutment surface roughness on plaque accumulation and peri-implant mucositis, *Clin. Oral Implants Res* 7 (1996) 201–211, 10.1034/j.1600-0501.1996.070302.x. [PubMed: 9151584]
- [41]. Heintze SD, Forjanic M, Ohmiti K, Rousson V, Surface deterioration of dental materials after simulated toothbrushing in relation to brushing time and load, *Dent. Mater* 26 (2010) 306–319, 10.1016/j.dental.2009.11.152. [PubMed: 20036418]
- [42]. Alexander-Katz R, Barrera RG, Surface correlation effects on gloss, *J. Polym. Sci. Part B Polym. Phys* 36 (1998) 1321–1334, 10.1002/(SICI)1099-0488(199806)36:8<1321::AID-POLB7>3.0.CO;2-U.
- [43]. O’Neill C, Kreplak L, Rueggeberg FA, Labrie D, Shimokawa CAK, Price RB, Effect of tooth brushing on gloss retention and surface roughness of five bulk-fill resin composites, *J. Esthet. Restor. Dent* 30 (2018) 59–69, 10.1111/jerd.12350. [PubMed: 29205770]
- [44]. Elbishari H, Silikas N, Satterthwaite JD, Is deterioration of surface properties of resin composites affected by filler size? *Int. J. Dent* 2020 (2020) 10.1155/2020/2875262.

HIGHLIGHTS

- The surface of conventional silica-based dental fillers was systematically functionalized with novel thiourethane oligomers.
- Incorporation of thiourethane-modified fillers dramatically reduced polymerization stress and uniformly increased composite fracture toughness.
- Thiourethane-modified composites demonstrated reduced surface roughness and lower gloss reduction after simulated toothbrushing.

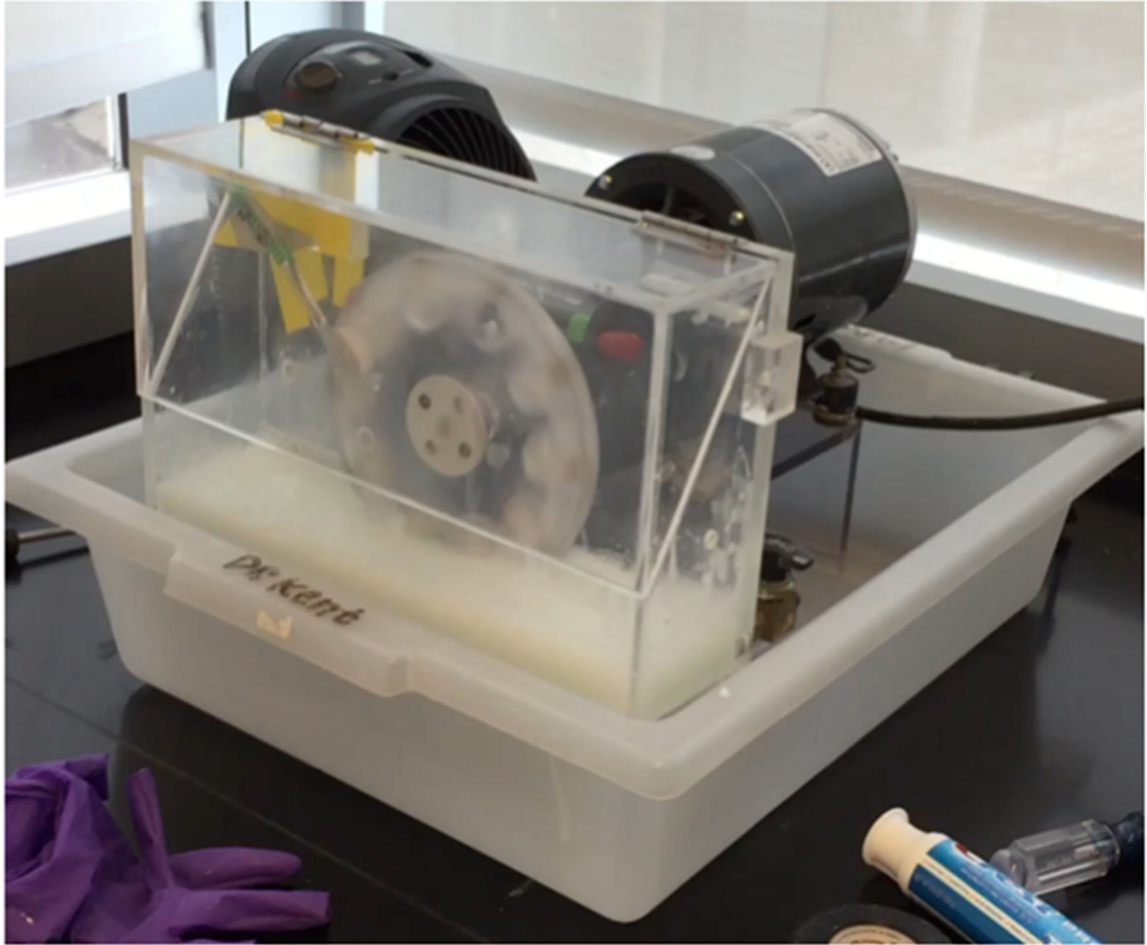


Fig. 1. Tooth brushing machine consisting of a drive motor, circular plate for epoxy-mounted composite samples, tooth brush and reservoir containing tooth paste solution.

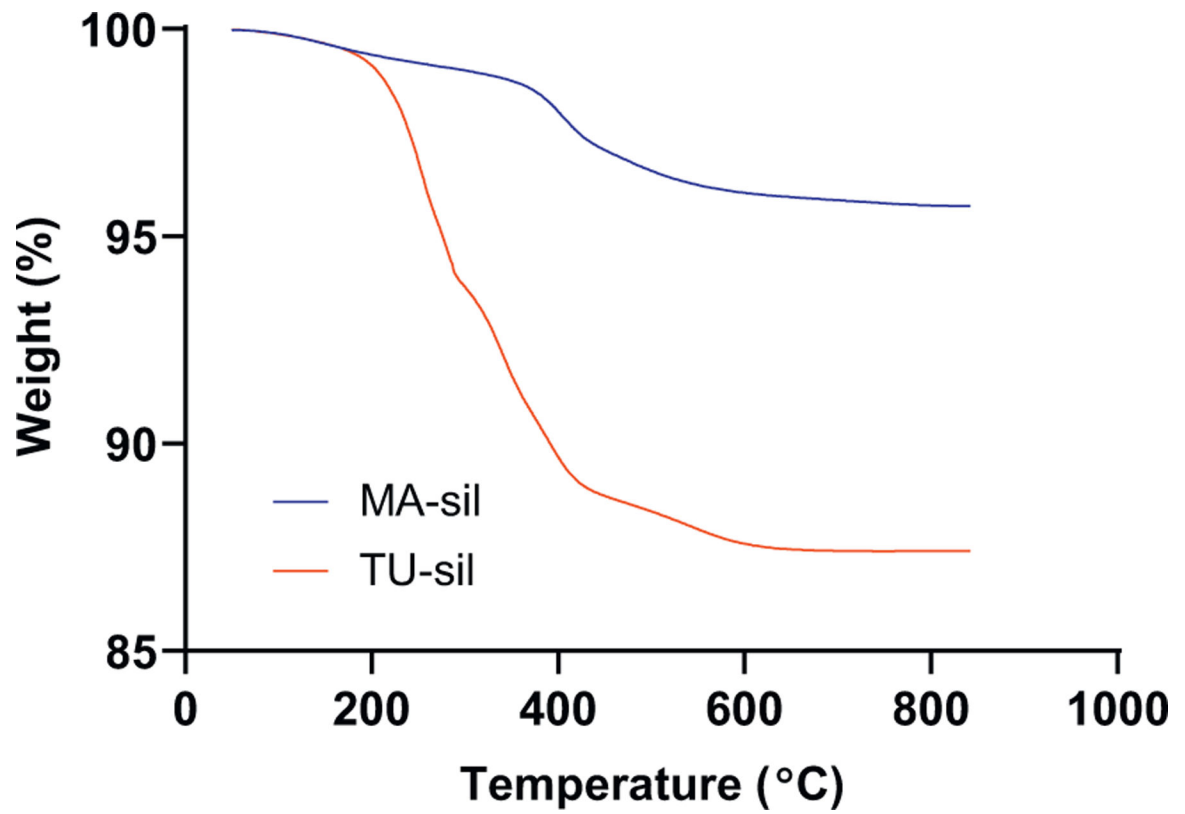


Fig. 2. Mass loss profiles measured by thermogravimetric analysis for methacrylate-silanized filler particles (control) and TU-silanized filler particles.

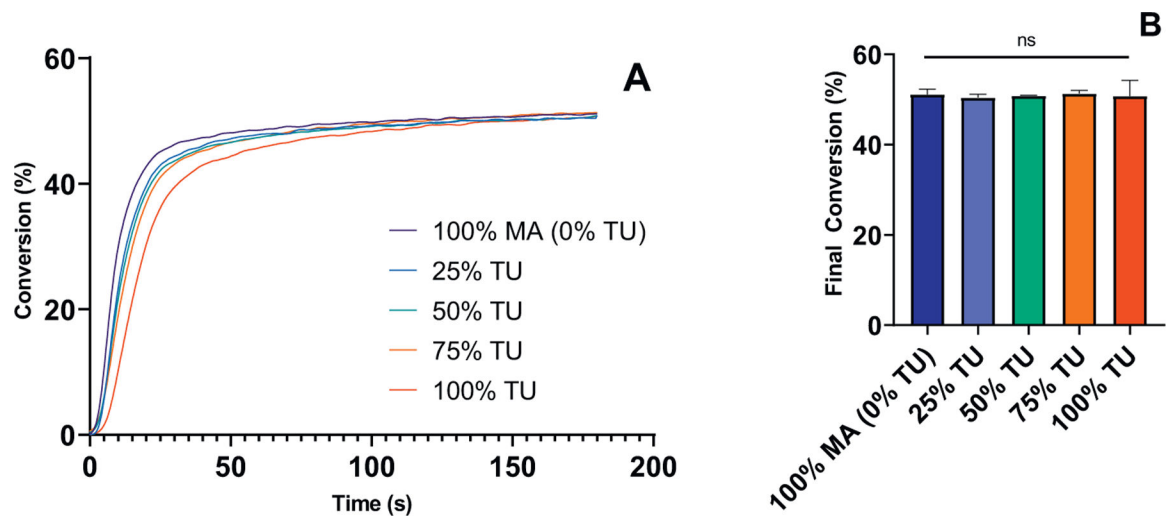


Fig. 3. Degree of conversion versus time (A) and final conversion (B, @ $t=180$ s) for all groups. Varying TU silane concentration did not affect the final degree of conversion.

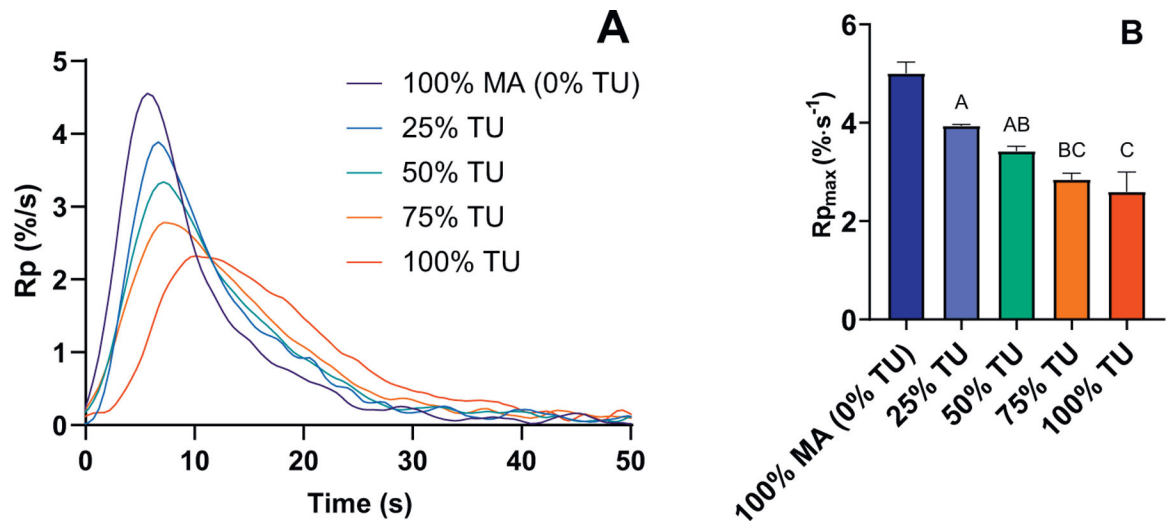


Fig. 4. Rate of polymerization (A, R_p) and maximum rate of polymerization (B, $R_{p_{max}}$) for all composites.

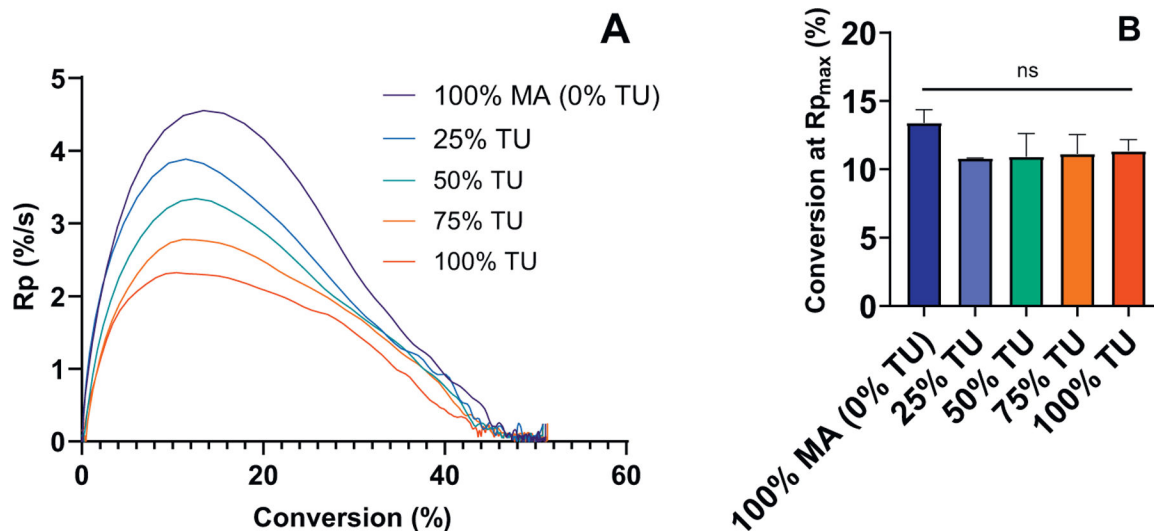


Fig. 5. Rate of polymerization (R_p) versus conversion (A) and corresponding degree of conversion at the maximum polymerization rate (B, $R_{p_{max}}$) for all groups.

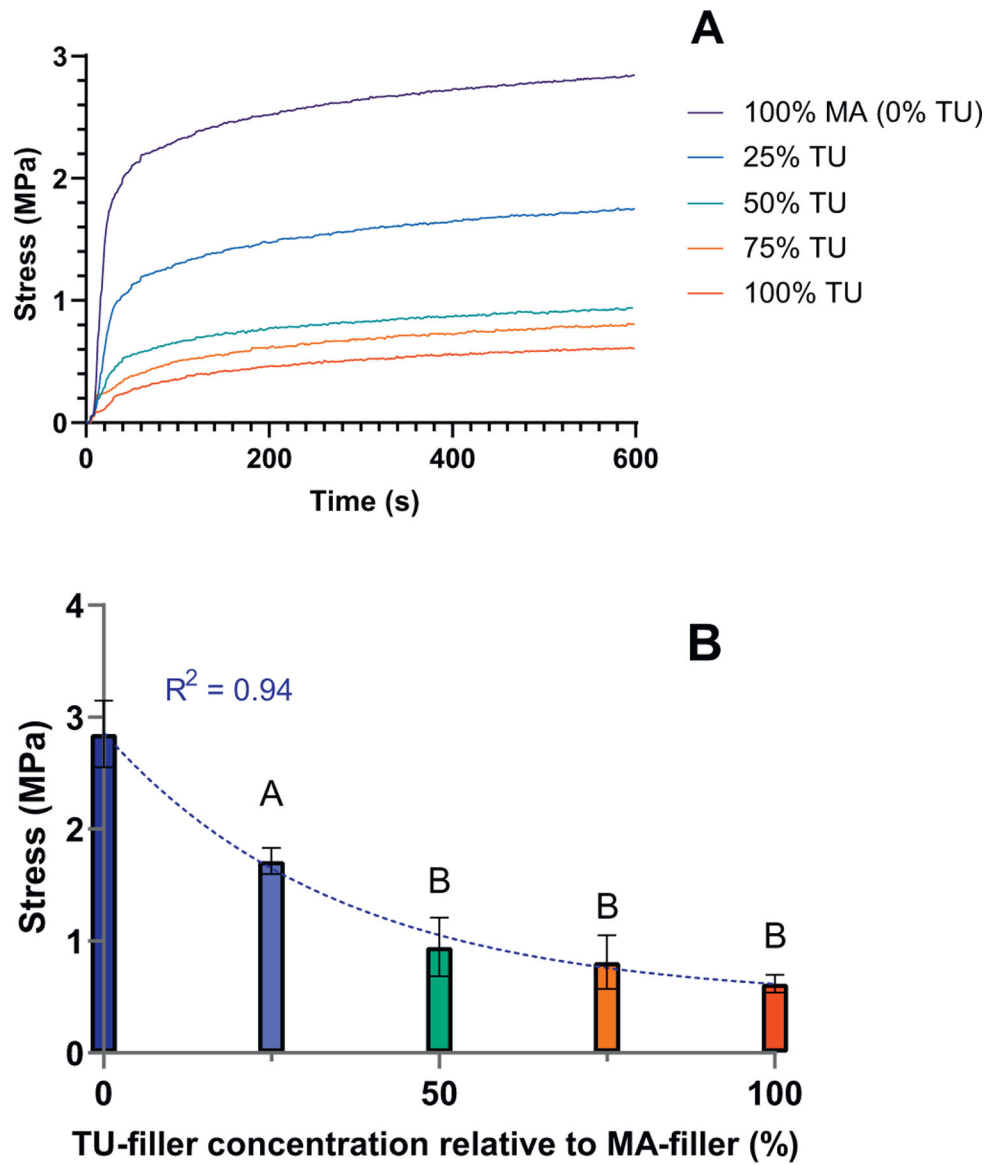


Fig. 6. Polymerization stress versus time for all composites (A) and nonlinear regression of polymerization stress at $t = 600$ s versus TU-filler concentration (B).

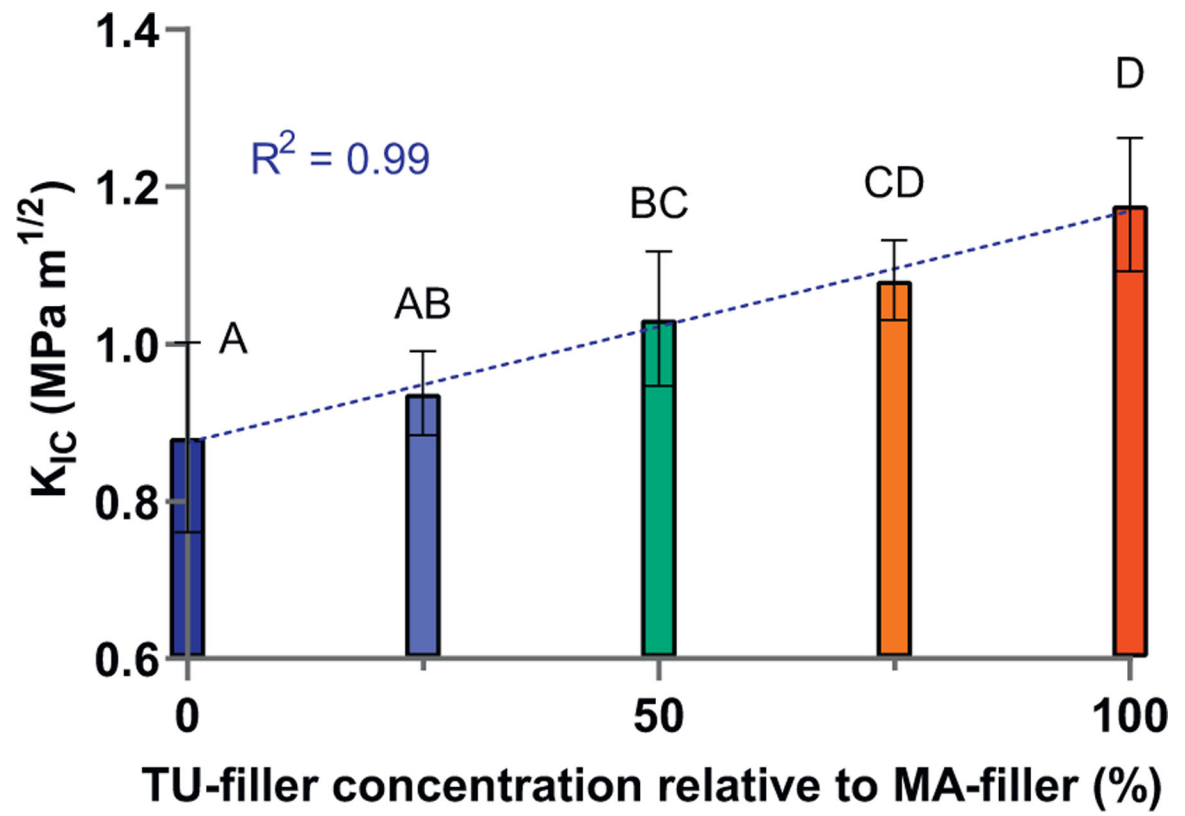


Fig. 7. Fracture toughness (K_{IC}) versus TU-to-MA filler ratio for all groups shown with corresponding linear regression.

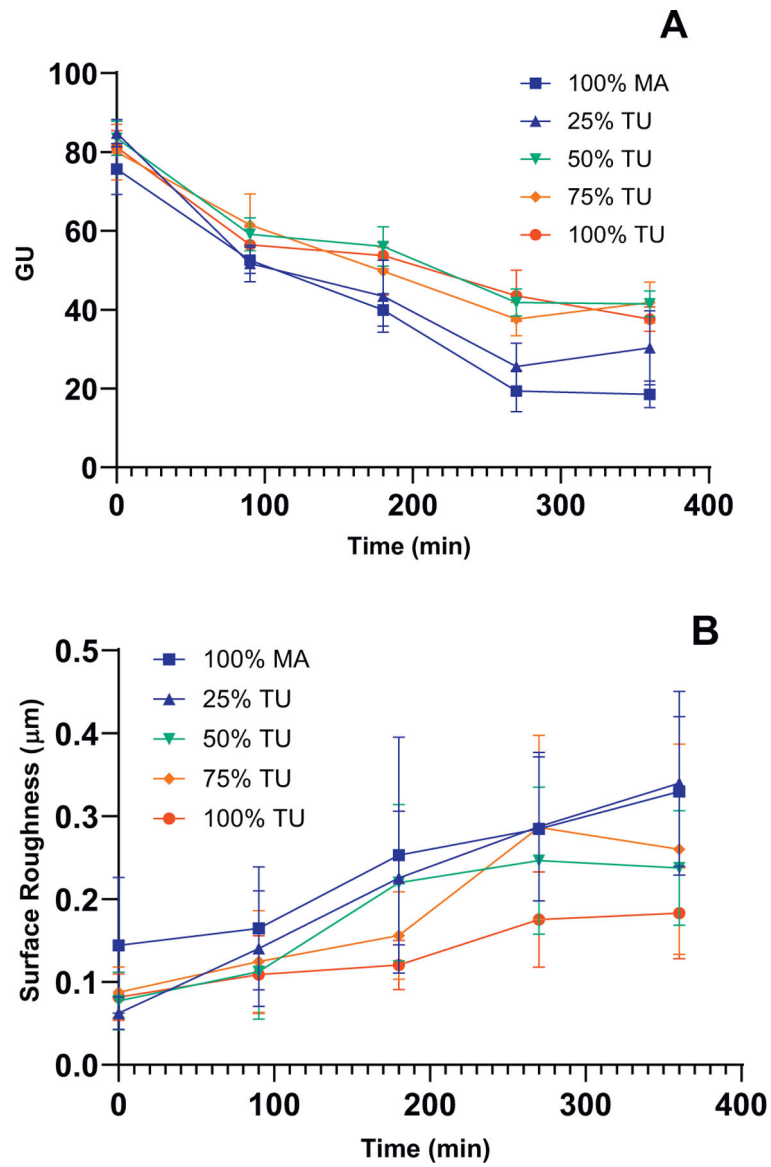


Fig. 8. Gloss (A) and surface roughness (B) for all composite groups. Measurements were taken every 90 min for a total of 360 min.

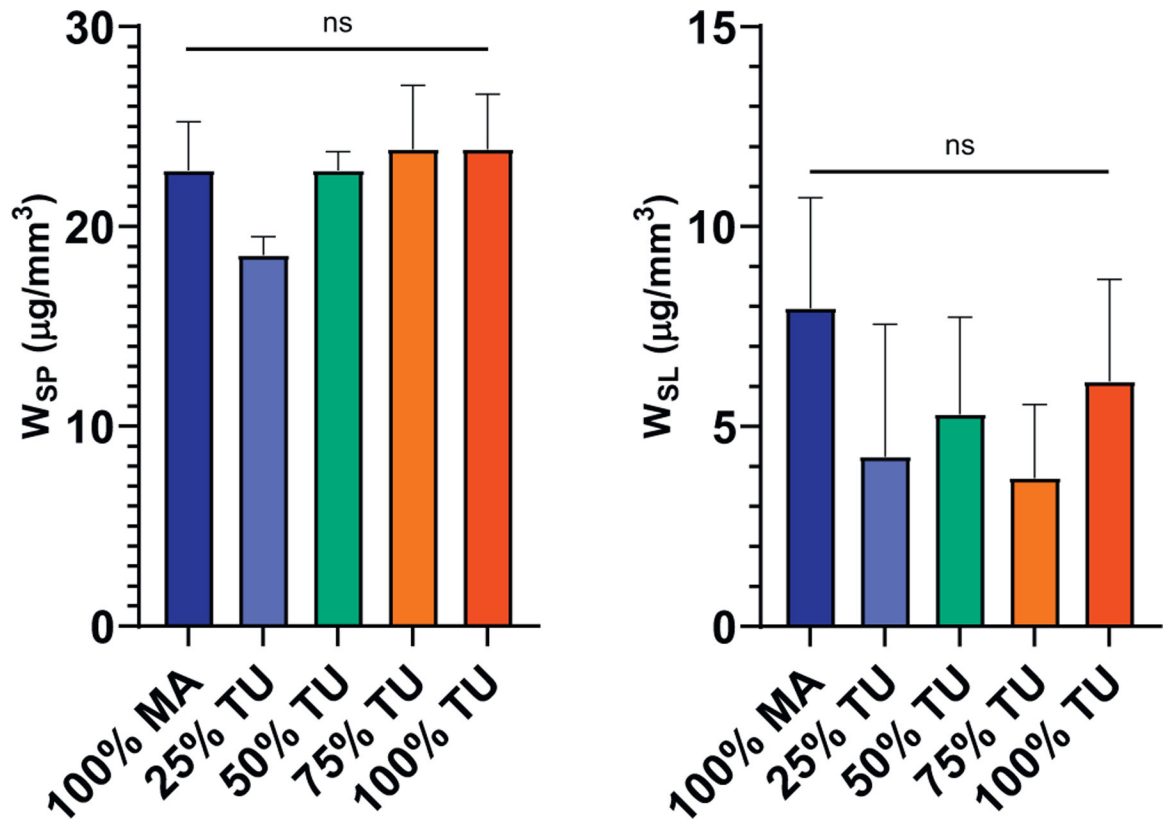


Fig. 9.
Water sorption (W_{SP}) and solubility (W_{SL}) for all composite groups.

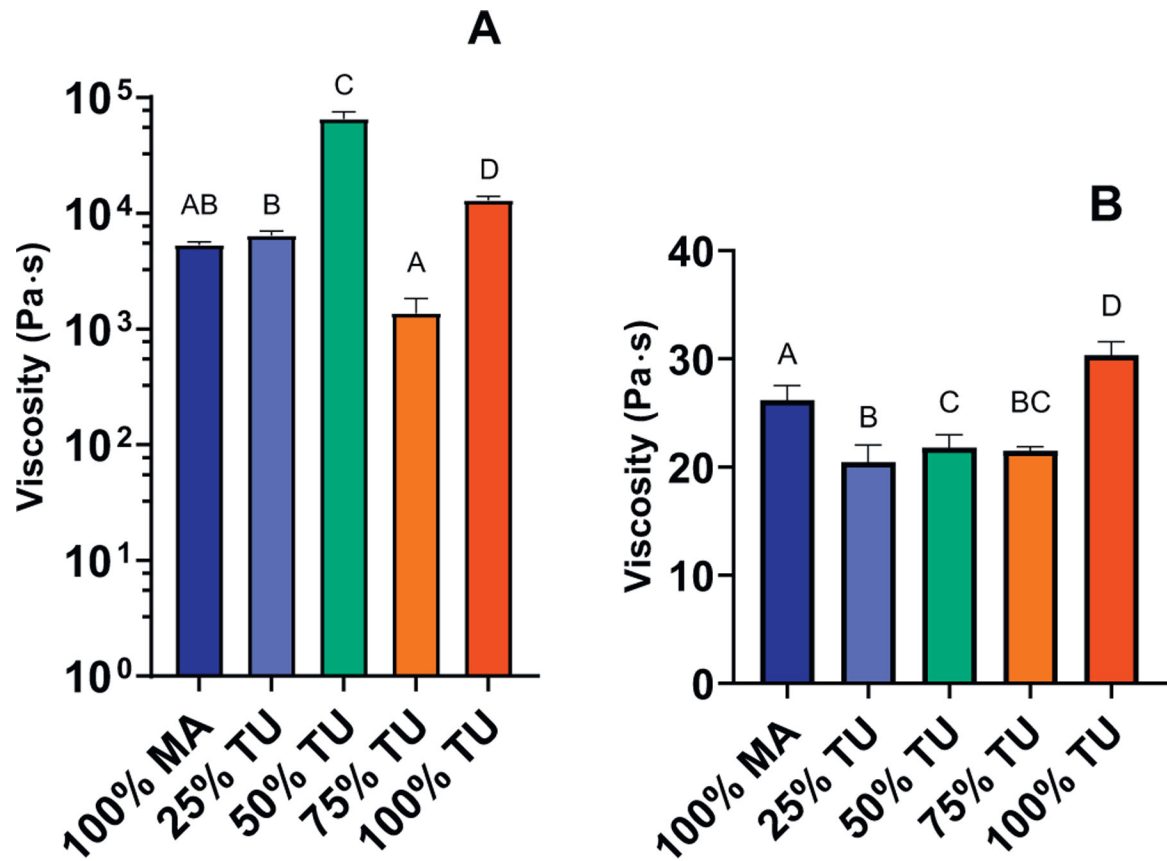


Fig. 10.

Graphs showing rheological properties for composite groups. Graph A shows composite paste viscosity results for all groups containing 70 wt% filler (OX50 plus MA and/or TU-silanized Ba filler). Graph B displays paste viscosity results for reduced-filler composites (50 wt% MA and/or TU-silanized Ba filler w/out OX50).

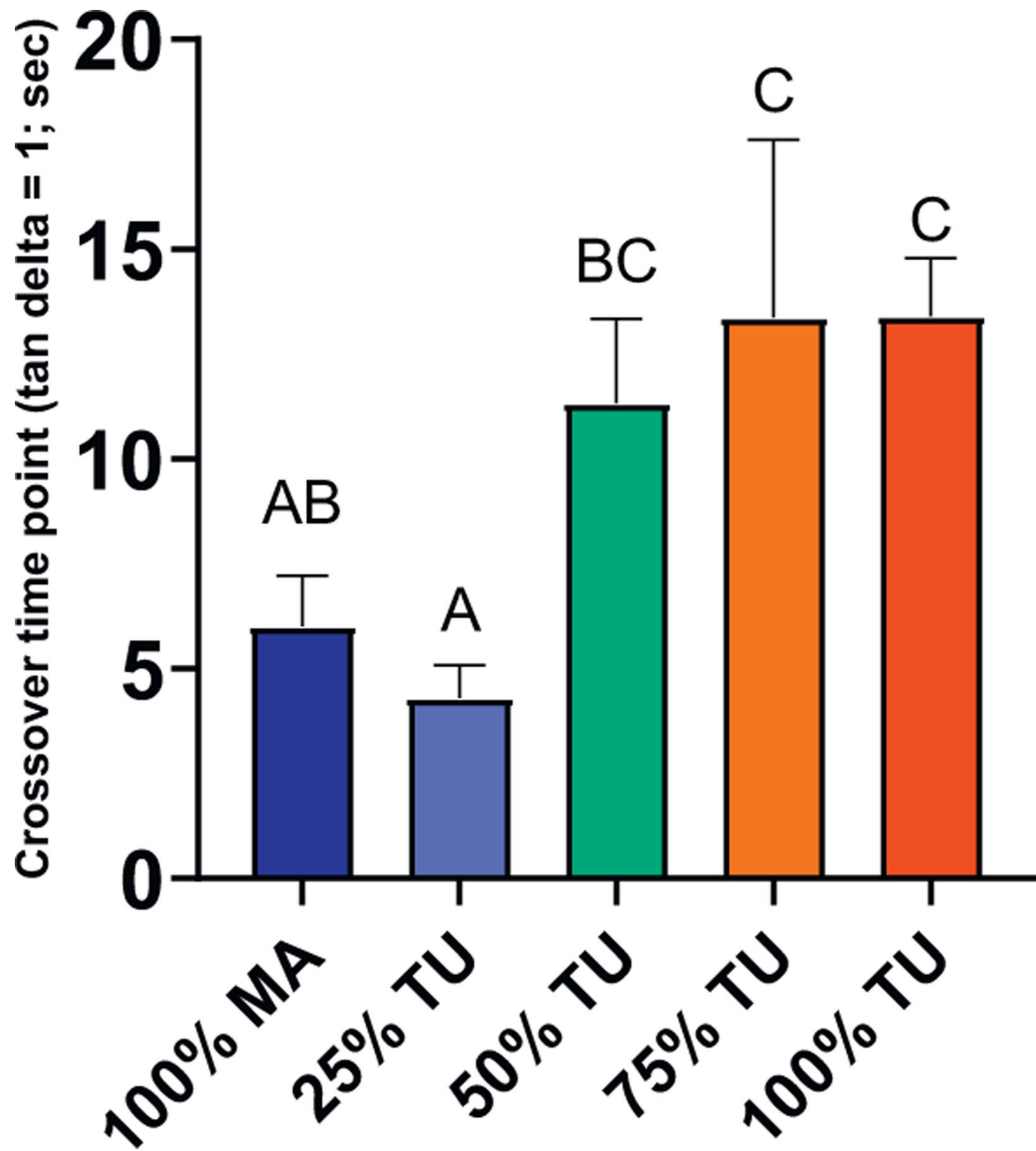


Fig. 11.
Time, in seconds, corresponding to the crossover modulus, where $\tan \delta = 1$, for all composite groups.

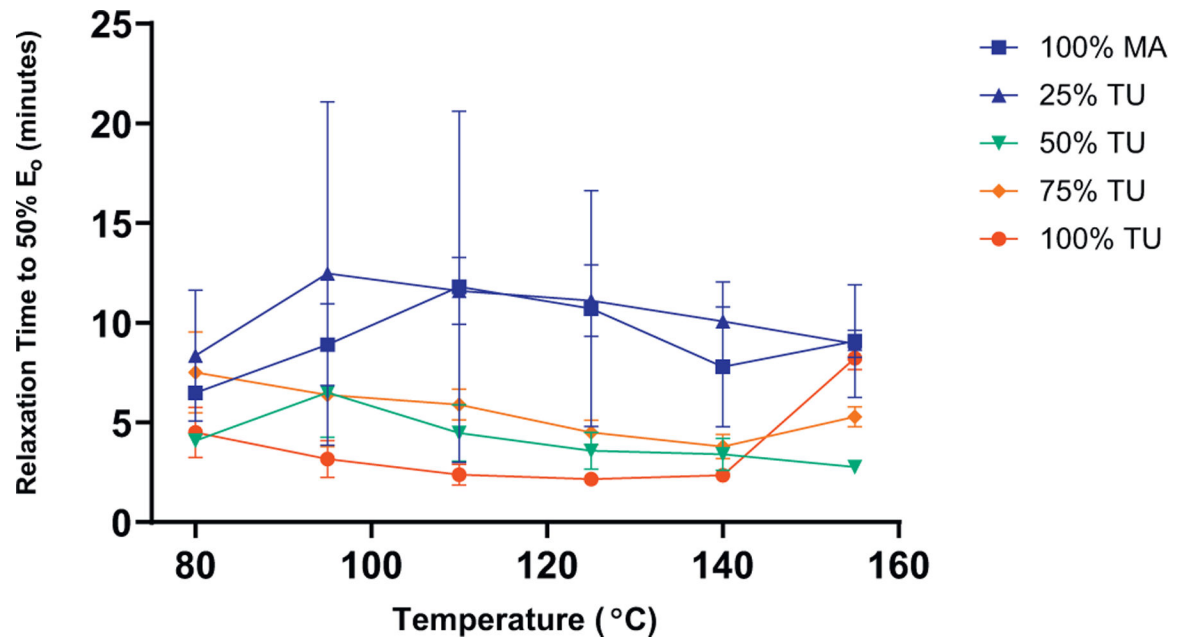


Fig. 12. Graph showing differences in stress relaxation times for all groups. Each data point represents the time required for each material to relax to 50% of the starting modulus, E_0 , as a function of increasing temperature.

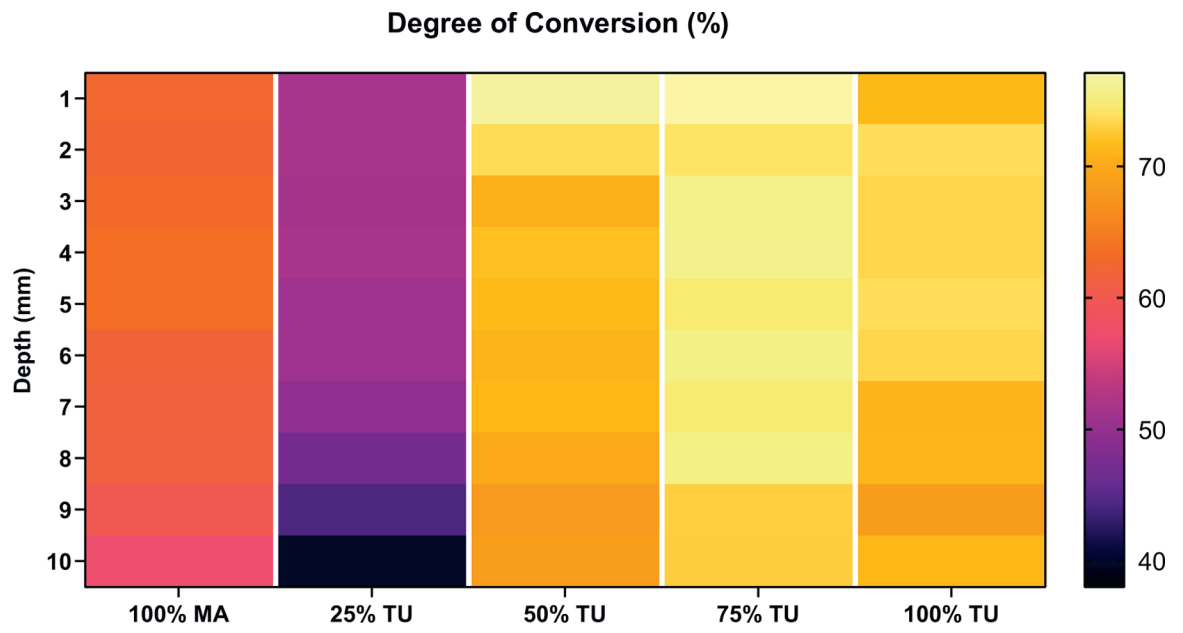


Fig. 13.
2D heatmap showing degree of conversion mapped with depth of cure for all composite groups.

Table 1

Resin-based-composite test groups organized according to filler type, where * denotes the control group.

| | 0.7μm silica glass filler (66.5 wt% of composite composition) | |
|----------|---|----------------------------------|
| | MA-silanized filler (wt%) | TU-silanized filler (wt%) |
| *100% MA | 100 | - |
| 25% TU | 25 | 75 |
| 50% TU | 50 | 50 |
| 75% TU | 75 | 25 |
| 100% TU | - | 100 |

Author Manuscript

Author Manuscript

Author Manuscript

Author Manuscript

Table 2

Comparison of weight fraction versus volume fraction of composite constituents for all groups. Silane mass was based on TGA results. Densities of MA silane, TU silane, OX50 and BUT resin were 1.045 g/mL, 0.9987 g/mL, 2.20 g/mL and 1.1324 g/mL, respectively [14,19]. Inorganic filler density (0.7 μm average particle size) was assumed to be 3 g/mL (exact value not available from manufacturer).

| Composite Group | Weight Fraction (wt%) | | | | Volume Fraction (vol%) | | | | | |
|-----------------|-----------------------|--------|--------|--------|------------------------|-----------------|--------|--------|--------|---------|
| | 100% MA (no TU) | 25% TU | 50% TU | 75% TU | 100% TU | 100% MA (no TU) | 25% TU | 50% TU | 75% TU | 100% TU |
| BUT Resin | 30 | 30 | 30 | 30 | 30 | 51.0 | 50.0 | 49.1 | 48.3 | 47.5 |
| OX50 | 3.5 | 3.5 | 3.5 | 3.5 | 3.5 | 3.1 | 3.0 | 3.0 | 2.9 | 2.8 |
| MA Filler | 63.7 | 47.8 | 31.9 | 15.9 | 0 | 40.8 | 30.1 | 19.7 | 9.7 | 0 |
| MA Silane | 2.8 | 2.1 | 1.4 | 0.7 | 0 | 5.1 | 3.8 | 2.5 | 1.2 | 0 |
| TU Filler | 0 | 14.5 | 29.1 | 43.6 | 58.1 | 0 | 9.1 | 18.0 | 26.5 | 34.7 |
| TU Silane | 0 | 2.1 | 4.2 | 6.3 | 8.4 | 0 | 4.0 | 7.8 | 11.5 | 15.0 |